

# Distribution of lesions and detection of influenza A(H5N1) virus, clade 2.3.4.4b, in ante- and postmortem samples from naturally infected domestic cats on U.S. dairy farms

Marta Mainenti,<sup>1</sup>  Christopher Siepkner,<sup>1</sup>  Drew R. Magstadt, Phillip Gauger,<sup>1</sup>   
David Baum,<sup>1</sup>  Barbara Petersen, Taylor Aubrey, Katie Sett, Eric R. Burroughs<sup>1</sup> 

**Abstract.** In March 2024, highly pathogenic avian influenza A(H5N1) virus, clade 2.3.4.4b, was detected in dairy cows in the United States, and at the same time in resident cats on affected farms. To help guide sample collection and diagnosis in cats, here we report the distribution of lesions and detection of H5N1 clade 2.3.4.4b influenza A virus (IAV) infection by PCR, immunohistochemistry (IHC), and serology in samples from 4 deceased and 2 living cats from 3 separate affected dairy farms. Although gross lesions were not diagnostic, histologically, all 4 deceased cats had nonsuppurative and necrotizing encephalitis and subtle interstitial pneumonia, and some also had significant myocarditis (3 of 4), chorioretinitis (2 of 4), and sialadenitis (1 of 2). The virus was detected by IHC in the aforementioned tissues, and by PCR in each brain (Ct=9.9–25.1), lung (17.4–32.7), oropharyngeal swab (28.3–30.5), urine (30.3–34.4), and nasal swab (33.5–34.1) collected postmortem; fecal swabs were PCR-negative. In the antemortem samples, the virus was detected by PCR in the oropharyngeal swabs (34.1–36.1), whole-blood samples (30.8–36.6), and one serum sample (31.7). Seroconversion was detected in one cat. Our results support histologic evaluation of brain, lung, eyes, and heart, and PCR testing of brain and lung for postmortem diagnosis, and show that oropharyngeal swabs, urine, serum, and whole blood are suitable samples for antemortem detection of IAV infection in clinically affected cats.

**Keywords:** avian; cats; clade 2.3.4.4b; encephalitis; highly pathogenic avian influenza; H5N1; influenza A virus; retinitis.

The Eurasian strain of highly pathogenic avian influenza (HPAI) A virus (IAV; *Orthomyxoviridae*, *Alphainfluenzavirus influenzae*) subtype H5N1, clade 2.3.4.4b, emerged at the end of 2021 in Europe<sup>20</sup> and is currently the dominant HPAI virus in the United States of America.<sup>7</sup> Since its first detection, this virus has caused multiple outbreaks in poultry and wild birds<sup>2,5,7</sup> with spillover infections and mortalities in a variety of terrestrial<sup>1,3,9,10,24,30</sup> and marine<sup>17,22</sup> mammal species in the Americas and Europe. In March 2024, in the northern Texas panhandle region, this virus was detected from multiple farms in milk and mammary gland tissue of dairy cows that had reduced feed intake, reduced rumination, and an abrupt drop in milk production.<sup>4</sup> At the same time, resident cats that were reportedly fed bovine raw colostrum and milk at the affected farms developed neurologic signs and unusually high mortality, which was confirmed to be due to the same virus strain.<sup>4</sup> To date, the H5N1 clade 2.3.4.4b virus has been detected in relatively few human cases,<sup>6,21,28</sup> some of whom were workers on affected dairy farms.<sup>6,28</sup>

The first detections of H5N1 2.3.4.4b HPAI in felids were reported in 2 bobcats<sup>10</sup> in the United States and 1 domestic

cat<sup>3</sup> in France in 2022, and in 3 domestic cats<sup>24</sup> in the United States and in 25 cats<sup>9</sup> in Poland in 2023; the felids developed severe systemic and neurologic disease or were found dead. Prior to the current outbreak in Europe and the United States, domestic cats<sup>11,13–16,23,25,27,29,31</sup> and larger felids, including tigers<sup>12,26</sup> and leopards,<sup>12</sup> around the globe have been known to be susceptible to H5 IAVs, including H5N1, both by natural<sup>11,12,14,16,25,26,31</sup> and experimental infection,<sup>13,15,23,29</sup> with development of a similar and often fatal disease. Historically, infection with H5N1 IAV in cats and other felids was mainly attributed to ingestion or direct and indirect contact with infected birds,<sup>3,12,14,18,27,31</sup> but cat-to-cat

Iowa State University Veterinary Diagnostic Laboratory, Ames, IA, USA (Mainenti, Siepkner, Magstadt, Gauger, Baum, Sett, Burroughs); Sunrise Veterinary Service, Amarillo, TX, USA (Petersen); New Ulm Regional Veterinary Center, New Ulm, MN, USA (Aubrey).

<sup>1</sup>Corresponding author: Marta Mainenti, Iowa State University Veterinary Diagnostic Laboratory, 1937 Christensen Dr, Ames, IA 50011, USA. mainenti@iastate.edu

transmission was also demonstrated in experimentally infected cats<sup>15,23</sup> and postulated in naturally infected tigers.<sup>26</sup>

Across recent<sup>10,24</sup> and previous<sup>12–15,23,25,27,29</sup> reports of H5N1 virus infection in cats and other felids, brain and lung appeared to be the organs most consistently and severely affected, with development of nonsuppurative and necrotizing encephalitis, interstitial pneumonia, diffuse alveolar damage, and vasculitis, as well as hemorrhages, congestion, or small foci of necrosis in various visceral organs. In reports of H5N1 2.3.4.4b in domestic cats<sup>3,9,24</sup> and bobcats,<sup>10</sup> this virus was consistently detected by PCR in the brain<sup>9,10,24</sup> and lung<sup>9,10</sup> of deceased cats and bobcats, as well as in nasal swabs and oropharyngeal swabs from the bobcats,<sup>10</sup> in 2 livers and a postmortem deep nasal swab from the cats in the United States,<sup>24</sup> in the postmortem tracheal and sinonasal swabs of the cat in France,<sup>3</sup> and in nasal swabs, throat swabs, and occasionally in liver, other internal organs, and rectal swabs in deceased and live cats in Poland.<sup>9</sup> Regarding viral antigen detection by immunohistochemistry (IHC), immunoreactivity was consistently found in the brain of all 3 cats in the United States,<sup>24</sup> and variably in the lung, heart, kidney, adrenal gland, myenteric plexus, and pancreas of the cats,<sup>24</sup> and in the brain of a bobcat.<sup>10</sup>

In natural<sup>14,25,31</sup> and experimental<sup>13,15,23,29</sup> infections in cats with other strains of H5N1 IAV, viral detection was confirmed by PCR, virus isolation, and/or IHC, mainly in the lung and brain, with variable detection in other organs and sample types such as liver, heart, kidney, spleen, adrenal gland, myenteric plexus, pancreas, intestine, mesenteric lymph node, tonsil, nasal conchae, rectal swab, oropharyngeal swab, serum, pleural fluid, and urine. In experimental studies with other H5N1 strains,<sup>13,23,29</sup> the virus was detected by viral isolation or PCR procedures in pharyngeal, nasal, and rectal swabs of cats as early as 1 d post-infection (dpi) and up to the end of the experiment at 7 dpi, regardless of the inoculation route (i.e., oculo-nasopharyngeal, intratracheal, alimentary, or horizontal).

Subclinical infection with H5N1 viruses has also been reported in natural and experimental infections.<sup>18,29</sup> During an outbreak in an animal shelter in Europe, H5N1 infection was detected by PCR in pharyngeal swabs in 3 of 40 cats and seroconversion in 2 cats that were in contact with infected birds.<sup>18</sup> Similarly, in a 2008 experimental study,<sup>29</sup> cats inoculated with lower doses of H5N1 virus ( $10^4$ ,  $10^2$ , and 1 embryo infectious dose [EID]) did not develop clinical signs, and seroconversion and viral detection occurred in the cats infected with  $10^4$  EID, but not in those inoculated with  $10^2$  or 1 EID.

Due to the implications of potential zoonotic and cross-species transmission of the HPAI H5N1 virus, a timely and accurate diagnosis in both live and dead animals, including companion animals is essential. Here, we report the distribution of lesions and detection of HPAI H5N1 clade 2.3.4.4b infection by PCR, IHC, and seroconversion in a variety of postmortem and antemortem samples collected from 6

naturally infected domestic cats associated with outbreaks in dairy cattle in Texas, New Mexico, and Minnesota in 2024. These results will help guide sampling, test selection, and interpretation in domestic cats suspected of being infected with H5N1 IAV.

## Materials and methods

The Iowa State University–Veterinary Diagnostic Laboratory (ISU-VDL; Ames, IA, USA) received 2 cats from Texas on 2024.03.21 (case 1; cats 1 and 2) and 2 cats from New Mexico on 2024.04.09 (case 2; cats 3 and 4) for autopsy, and antemortem clinical samples from 2 live, clinically ill cats (case 3; cats 5 and 6) from Minnesota on 2024.06.10 for diagnostic evaluation. All 6 animals were adults residing on 3 separate dairy farms on which cattle were diagnosed with H5N1 IAV clade 2.3.4.4b infection. The deceased cats from Texas and New Mexico (cats 1–4) were 6- to 24-mo-old; the live cats from Minnesota (cats 5 and 6) were 5- and 13-y-old, respectively. Although infection in the Texas cats (cats 1 and 2) was reported previously,<sup>4</sup> this is the first report focusing on the cats originating from New Mexico and Minnesota (cats 3–6). Similarly to the cats from Texas, the cats residing on the New Mexico farm (cats 3 and 4) were part of a larger colony of cats that foraged on mice, rats, and birds, and were also offered raw and pasteurized colostrum and milk from sick cows that was being diverted from the bulk commercial milk. Cats 5 and 6 from Minnesota were indoor cats that were reported to only have contact with people working at the affected dairy farm.

All cats from Texas and New Mexico (cats 1–4) experienced various degrees of neurologic signs, including lethargy, inappetence, weakness, depression, ataxia, stumbling, lack of awareness, dullness, and inability to rise. Blindness, reduced menace reflex, and ocular and nasal discharge were also reported. Duration of illness was 24–48 h from when clinical signs were first observed, with progressively more severe neurologic signs before death. Cats 1–3 died naturally; cat 4 was euthanized by gunshot on farm due to presumed H5N1 IAV infection and concerns for potential human exposure during restraint. All samples in cats 1–4 were collected postmortem. Regarding the cats from Minnesota, cat 5 developed clinical signs first, followed by cat 6 on the next day. Clinical signs were bilateral ocular and nasal discharge, pyrexia, tachypnea, dehydration, and lethargy. To our knowledge, cat 5 recovered clinically and was still alive at the time of manuscript submission; cat 6 had a rapid progression of illness and died 5 d after the onset of clinical disease and sample collection. Samples were collected from cats 5 and 6 on the day of onset of clinical signs in cat 6.

Sections of brain, eye, lung, heart, spleen, liver, lymph node, and kidney were systematically collected from all cats submitted for autopsy (cases 1 and 2; cats 1–4) and placed in 10% neutral-buffered formalin for histologic evaluation. Nasal turbinates, cribriform plate, lacrimal glands, salivary

glands, trachea, pharynx, esophagus, stomach, pancreas, small and large intestine, skeletal muscle, thyroid glands, adrenal glands, and lymph node were also collected from cats 3 and 4. Additional samples from cat 3 included tonsils, larynx, optic chiasm, pituitary gland, sciatic nerve, urinary bladder, uterus, ovaries, mammary gland, and bone marrow. The cerebrum was retrieved from all cats; the cerebellum and brainstem were not available for cat 4 euthanized by gunshot. Formalin-fixed tissues were routinely trimmed, processed, and sectioned at 4  $\mu\text{m}$  for H&E staining and microscopic evaluation. IHC targeting the IAV nucleoprotein (NP) was performed as described previously.<sup>4</sup> Sections of swine lung positive for IAV infection by reverse-transcription real-time PCR (RT-rtPCR) were used as positive controls. Sections of brain, lung, and eye from Iowa cats diagnosed with an unrelated disease before the recent H5N1 IAV detection in dairy cattle were used as negative controls.

Fresh samples of brain and lung were collected from all cats for IAV RT-rtPCR targeting the matrix and NP genes, followed by H5 and 2.3.4.4b subtyping RT-rtPCR assays. The following samples were also collected from cats 3 and 4 during autopsy for RT-rtPCR testing: oropharyngeal swab, nasal swab, fecal swab, and urine. The oropharyngeal swabs from cats 3 and 4 were collected in duplicate using sterile polyester swabs (Fisher Scientific): 1 swab was placed in 2 mL of 1 $\times$  PBS (Fisher Scientific), and 1 swab in 5 mL of brain-heart infusion (BHI) broth (Becton Dickinson). The fecal swabs were placed in PBS as described above. Urine was collected via cystocentesis using a sterile syringe and a 20-ga needle during the autopsy procedure. The same set of samples was also collected from 2 additional cats received for rabies testing (cats 7 and 8), to serve as negative controls. In cats 5 and 6, oropharyngeal swabs, EDTA whole blood, and serum were collected antemortem. The RT-rtPCR used to screen for the presence of IAV RNA was performed following a NAHLN-approved assay with deviations that included the VetMAX Gold SIV detection kit (Fisher Scientific), as described previously.<sup>4</sup> Samples with cycle threshold (Ct) values <40.0 were considered positive. Following the IAV RT-rtPCR screening, positive samples were further analyzed via NAHLN-approved H5 subtyping and a Eurasian lineage goose/Guangdong clade 2.3.4.4b-specific RT-rtPCR using the same RNA extract, according to standard operating procedures. Positive RNA extracts from each cat were also submitted to the National Veterinary Services Laboratories (NVSL; Ames, IA, USA) for confirmation and further characterization.

We used a commercial ELISA (Swine influenza virus antibody test kit; Idexx) according to the manufacturer's instructions to detect circulating antibodies to IAV NP in serum samples from cats 5 and 6. Briefly, samples were diluted 10-fold in sample diluent; 100  $\mu\text{L}$  of undiluted negative control (NC) and 100  $\mu\text{L}$  of undiluted positive control were dispensed into duplicate wells of the avian IAV NP antigen-coated plates; 100  $\mu\text{L}$  of diluted samples were

dispensed into their appropriate wells and incubated for 60 min at room temperature (RT). After incubation, each well was washed with  $\sim 350 \mu\text{L}$  of 1 $\times$  wash solution 3–5 times (wash step). Plates were washed with 3 cycles from an automatic washer. A cycle was defined as an aspiration and then a dispensing. Next, 100  $\mu\text{L}$  of conjugate was dispensed into each well, covered, and incubated for 30 min at RT. TMB substrate was then dispensed into each well, covered, and incubated in the dark for 15 min at RT. This was followed by dispensing 100  $\mu\text{L}$  of stop solution into each well. The plates were read at 650 nm. This assay was validated at the ISU-VDL in bovine and swine samples and was not previously validated in cats; signal:noise ratio (S:N) values <0.6 are considered positive for bovine and porcine serum samples.

## Results

Part of the diagnostic investigation conducted on cats 1 and 2 was published previously.<sup>4</sup> Here we provide more detail of the histologic and immunohistochemical findings in cats 1 and 2 and a comparison of all diagnostic results with those of cats 3–6.

At postmortem evaluation, all cats appeared to be in adequate body condition. Autolysis was mild in cats 1–3 and moderate in cat 4. Gross findings in all cats were mild and nonspecific, and included mild subcutaneous and meningeal hemorrhage in cats 1 and 2, and no-to-low content in the gastrointestinal tract in all cats. Cat 4 also had a gunshot wound in the skull.

The most consistent histologic lesions across cats from both outbreaks were mononuclear and necrotizing encephalitis (4 of 4 cats), interstitial pneumonia (4 of 4), and chorioretinitis (2 of 4; Table 1). The encephalitis was multifocal and severe in all cats and consisted of random foci of perivascular lymphocytic inflammation, necrotizing vasculitis, gliosis, and neuronal necrosis within the white and gray matter (Fig. 1A, 1B). Lesions were most consistently found in the cerebrum (4 of 4) and brainstem (3 of 3). In addition, moderate perivascular inflammation also extended to the leptomeninges in the cerebrum of cats 1–3. No lesions were found in the cerebellum except for mild perivascular inflammation in the white matter of the cerebellar peduncle of cat 3. The pneumonia consisted of small random foci of lymphocytic and fibrinous inflammation within alveolar septa, with septal necrosis and alveolar edema (4 of 4; Fig. 1C). One eye in cat 2 and both eyes in cat 3 were affected by segmental lesions consisting of perivascular lymphocytic retinitis with loss of nerve fibers, rarefaction, ganglion cell necrosis, attenuation of the inner plexiform layer, jumbling and loss of nuclear layers, photoreceptor necrosis, and retinal detachment (2 of 4; Fig. 1D). Similar lymphocytic perivascular inflammation was also present around the choroid vasculature (2 of 4). Retinal lesions were more severe and disseminated, with the accumulation of fibrin, hemorrhages, and edema in the retina of cat 3 (Fig. 1C). Low numbers of lym-

**Table 1.** Location of histologic lesions and immunoreactivity (IHC) for influenza A virus nucleoprotein in cats naturally infected with influenza A(H5N1) virus from Texas and New Mexico.

Location	Presence or absence of lesions/IHC results				No. of cats with lesions	No. of cats IHC+
	Cat 1 (case 1)	Cat 2 (case 1)	Cat 3 (case 2)	Cat 4 (case 2)		
Brainstem	++	++	++	NA	3/3	3/3
Cerebellum	--	--	+-	NA	1/3	0/3
Cerebrum	++	++	++	++	4/4	4/4
Spinal cord	NA	NA	+-	NA	1/1	0/1
Peripheral nerves	NA	NA	--	NA	0/1	0/1
Eye (retina, choroid)	--	++	++	--	2/4	2/4
Ocular conjunctiva	NA	NA	--	--	0/2	0/2
Eyelid conjunctiva	NA	NA	--	+-	1/2	0/2
Lacrimal gland	NA	NA	--	--	0/2	0/2
Nasal turbinates	NA	NA	--	+-	1/2	0/2
Cribriform plate	NA	NA	--	+-	1/2	0/2
Larynx	NA	NA	--	NA	0/1	0/1
Trachea	NA	NA	--	--	0/2	0/2
Lung	++	++	+-	+-	4/4	2/4
Tonsil	NA	NA	+-	NA	1/1	0/1
Lymph node	NA	NA	--	--	0/2	0/2
Spleen	--	--	--	--	0/4	0/4
Submandibular salivary gland	NA	NA	++	+-	2/2	1/2
Minor salivary glands—pharynx	NA	NA	NA	+-	1/1	0/1
Minor salivary glands—tongue	NA	NA	++	NA	1/1	1/1
Parotid gland	NA	NA	--	+-	1/2	0/2
Sublingual salivary glands	NA	NA	--	NA	0/1	0/1
Tongue	NA	NA	--	NA	0/1	0/1
Esophagus	NA	NA	--	--	0/2	0/2
Stomach	NA	NA	--	--	0/2	0/2
Large intestine	NA	NA	--	--	0/2	0/2
Small intestine	NA	NA	--	--	0/2	0/2
Heart	++	++	+-	--	3/4	2/4
Skeletal muscle	NA	NA	--	--	0/2	0/2
Liver	--	--	+-	--	1/4	0/4
Kidney	--	--	--	--	0/4	0/4
Urinary bladder	NA	NA	--	NA	0/1	0/1
Adrenal gland	NA	NA	+-	--	1/2	0/2
Parathyroid gland	NA	NA	--	NA	0/1	0/1
Thyroid gland	NA	NA	+-	--	1/2	0/2
Pancreas	NA	NA	--	--	0/2	0/2
Ovary	NA	NA	--	NA	0/1	0/1
Uterus	NA	NA	--	NA	0/1	0/1
Bone marrow	NA	NA	--	NA	0/1	0/1

+ = lesion present or positive IHC; -- = lesion absent or negative IHC; NA = not available.

phocytes and plasma cells also extended into the ciliary body, processes, and cleft, as well as iris, sclera, and eyelid conjunctiva of cat 3, mainly in a perivascular location. No microscopic lesions were seen in the lacrimal glands (0 of 2) and the ocular conjunctiva (0 of 4).

Additional microscopic lesions included mononuclear and necrotizing myocarditis in 3 of 4 cats (Fig. 1E), mild necrotizing and neutrophilic hepatitis (1 of 4), focal necrosis in the adrenal gland (1 of 4), and mild lymphocytic perivascular inflammation

in multiple tissues, such as thyroid gland (1 of 4), parotid gland (1 of 2), submandibular salivary gland (2 of 2), and minor salivary glands of the pharynx (1 of 1). Cat 3 also had severe necrotizing tonsillitis and mild-to-moderate lymphocytic and necrotizing inflammation of the submandibular salivary gland and minor salivary glands of the tongue (Fig. 1F). Cat 4 also had neutrophilic, lymphocytic, and histiocytic rhinitis.

On IHC, immunoreactivity for IAV NP was detected in the nucleus and cytoplasm of several cell types and in multiple



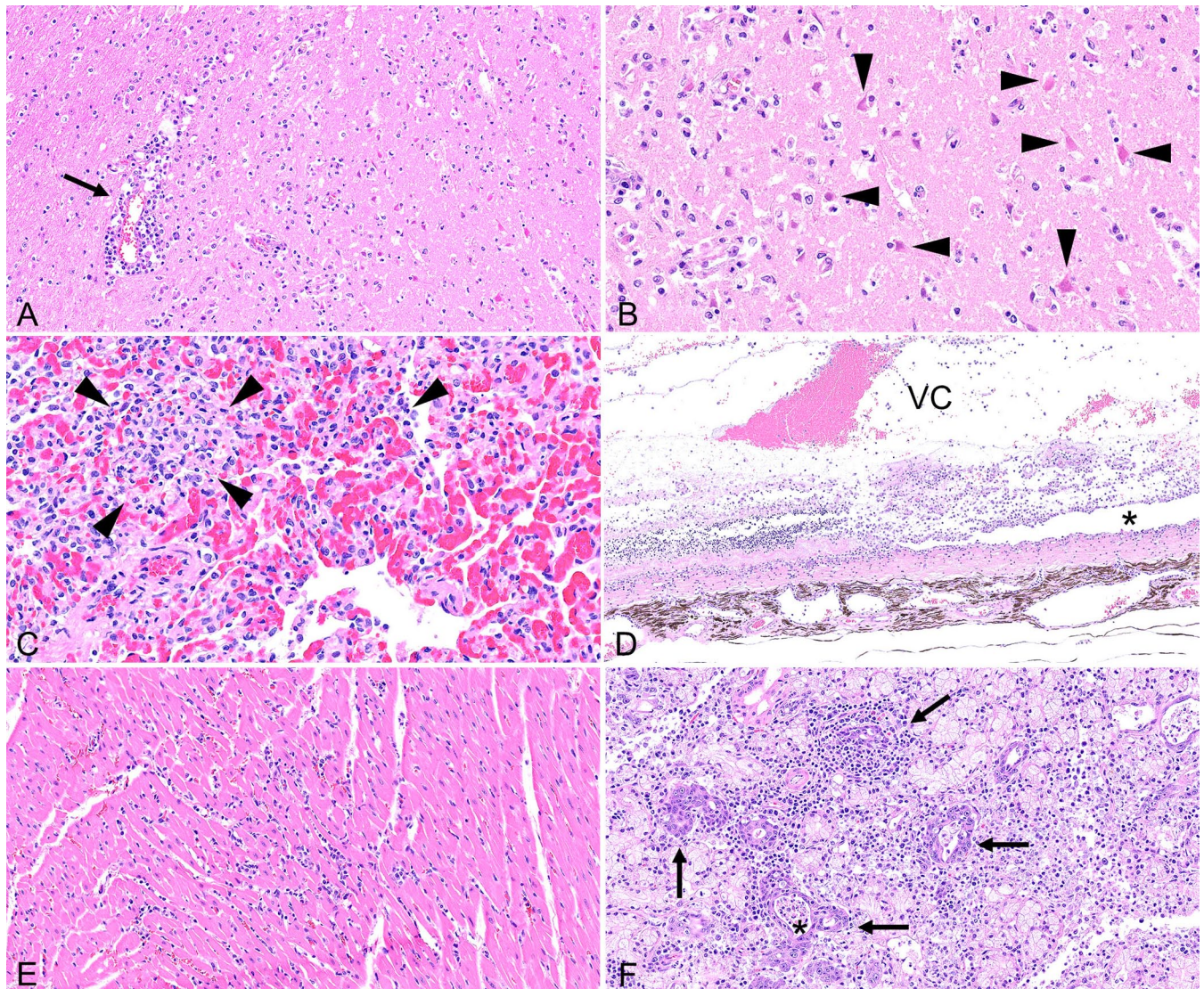


**Figure 1.** Highly pathogenic avian influenza A(H5N1) virus clade 2.3.4.4.b infection in domestic cats. **A.** Multifocal necrotizing encephalitis with vasculitis (arrow) and gliosis within cerebral cortex. Blood vascular tunics are obscured by mononuclear inflammation. **B.** Acute neuronal necrosis (shrunken, angular, hyper-eosinophilic pyramidal neurons; arrowheads) and gliosis within the cerebral neuropil. **C.** Acute multifocal necrotizing interstitial pneumonia with alveoli containing fibrin, neutrophils, and necrotic cellular debris (arrowheads). **D.** Segmental, necrotizing chorioretinitis with retinal vasculitis and loss of nerve fibers, ganglion cell, plexiform, and nuclear layers. Photoreceptors are abruptly lost with retinal detachment (asterisk). An exudate of fibrin, hemorrhage, neutrophils, and macrophages is present within the vitreous chamber (VC). **E.** Acute interstitial myocarditis with cardiac myocyte degeneration and necrosis. **F.** Sialadenitis within a submandibular salivary gland with a mononuclear inflammatory infiltrate, degeneration and necrosis of the salivary gland epithelium (arrows), and intraluminal necrotic debris (asterisk).

organs intralesionally: neurons (4 of 4 cats; Fig. 2A, 2B); bronchiolar epithelium (1 of 4), necrotic cells within alveolar spaces and septa (2 of 4), and septal mononuclear cells in the lung (2 of 4; Fig. 2C); all layers of the retina (2 of 4; Fig. 2D); cardiomyocytes (2 of 4; Fig. 2E); the epithelium of a submandibular salivary gland (1 of 2; Fig. 2F), and minor salivary glands of the tongue (1 of 1). In cat 3, small foci of immunoreactivity in cellular debris lining the mucosal epithelium of the large intestine were also suspected, although no significant

lesions were observed in the intestinal mucosa and lamina propria on H&E. All other examined tissue sections had no immunoreactivity (Table 1).

Brain and lung from all cats were positive by IAV screening RT-rtPCR with low Ct values in cats 1 and 2 from Texas (9.9, 13.5 on brain; 17.4, 24.4 on lung), and medium-to-high Ct values in cats 3 and 4 from New Mexico in the same organs (21.2, 25.1 on brain; 32.5, 32.7 on lung; Table 2). IAV nucleic acid was also detected at relatively high Ct values in



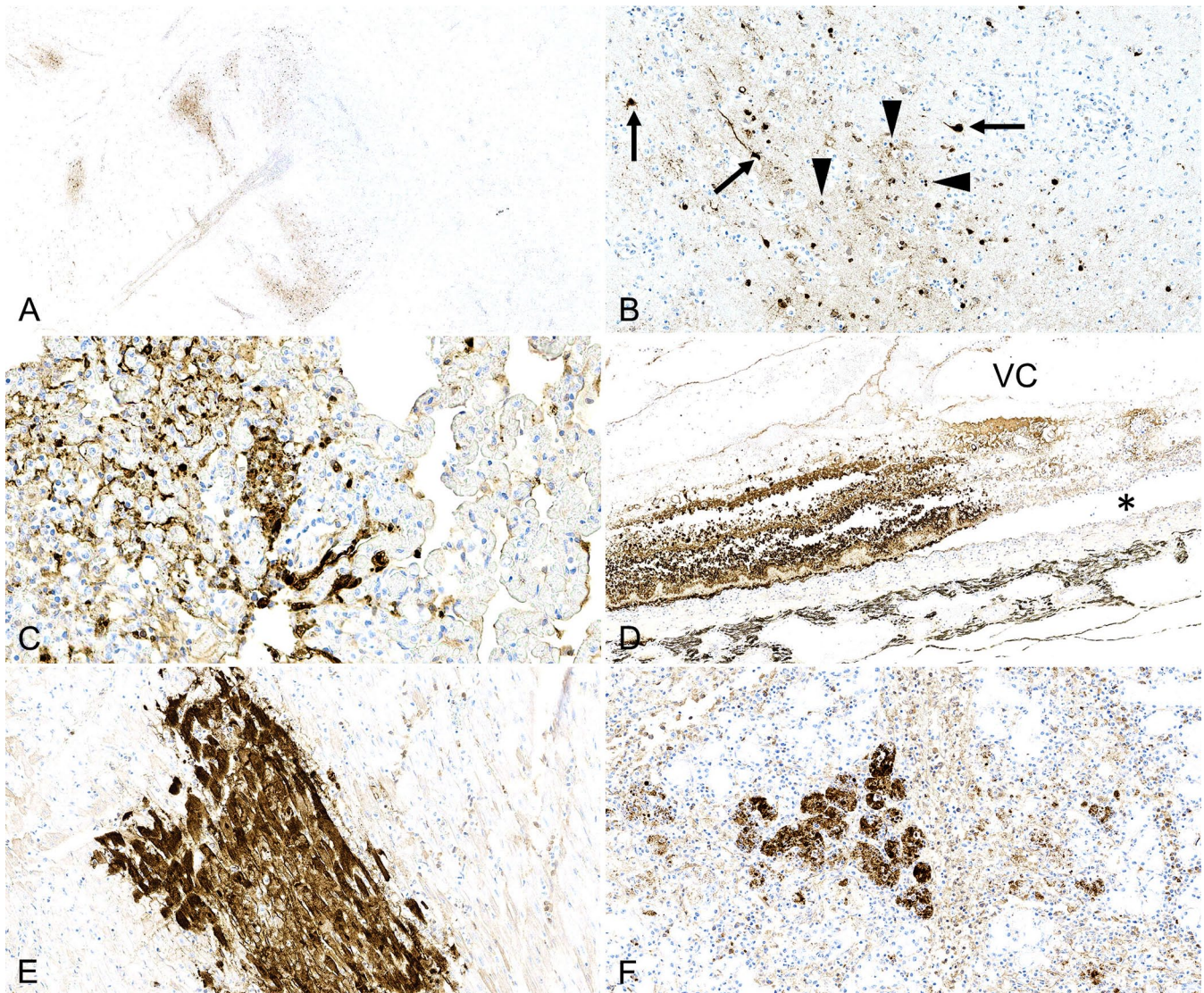


**Figure 2.** Immunohistochemistry for influenza A virus nucleoprotein in cats infected with highly pathogenic avian influenza A(H5N1) virus clade 2.3.4.4.b. **A.** Multifocal distribution of immunoreactivity within the cerebral cortex. **B.** Pyramidal neurons and axons have strong, intracytoplasmic and intranuclear immunoreactivity (arrows). The neuropil is populated and infiltrated by numerous immunoreactive glial and inflammatory cells (arrowheads). **C.** Cells within alveolar spaces and septa of the lung have strong intracytoplasmic and intranuclear immunoreactivity. **D.** Strong, segmental, intracellular, and intranuclear immunoreactivity of all cell layers of the retina with separation from the underlying choroid (asterisk). VC = vitreous chamber. **E.** Well-demarcated area with strong intrasarcoplasmic immunoreactivity within cardiac myocytes. **F.** Strong, multifocal, intracytoplasmic, and intranuclear immunoreactivity in the submandibular salivary gland epithelium.

the oropharyngeal swabs, nasal swabs, and urine from cats 3 and 4, with the lowest Ct values in oropharyngeal swabs collected in PBS (28.3, 30.5), followed by oropharyngeal swabs collected in BHI (31.3, 32.3), urine (30.3, 34.4), and nasal swabs (33.5, 34.1; Table 2). Fecal swabs were negative in both cats. In cats 5 and 6, IAV nucleic acids were detected at relatively high Ct values in the oropharyngeal swabs (36.1 and 34.1, respectively) and EDTA whole blood (36.6 and 30.8, respectively) in both cats, and in the serum from cat 6 with a Ct of 31.7 (Table 2). The H5 subtype- and clade

2.3.4.4b-specific RT-rtPCR assays were also positive in each positive sample, with Ct values consistent with the IAV RT-rtPCR, with the exception of lung from cat 3, nasal swabs from cats 3 and 4, and oropharyngeal swab from cat 5 (Table 2). Positive samples from each cat were submitted to NVSL for confirmation and further characterization; an H5N1 HPAI virus of the Eurasian lineage goose/Guangdong H5 clade 2.3.4.4b was confirmed in all cats. All samples from cats 7 and 8 used as negative controls tested negative by IAV RT-rtPCR. Serologically, circulating antibodies to IAV

**Table 2.** Results of RT-rfPCR for influenza A virus, H5 subtype, and H5 2.3.4.4b clade expressed as cycle threshold (Ct) values in naturally infected cats.

Animal	State	IAV PCR test	Brain	Lung	Urine	Oropharyngeal swab†	Nasal swab	Fecal swab	EDTA blood	Serum	
Cat 1 (case 1)	TX	IAV	9.9*	17.4*	NA	NA	NA	NA	NA	NA	
		H5 subtype	10.7*	16.5*							
		H5 2.3.4.4b	11.9*	18.0*							
Cat 2 (case 1)	TX	IAV	13.5*	24.4*	NA	NA	NA	NA	NA	NA	
		H5 subtype	14.0*	23.8*							
		H5 2.3.4.4b	15.2*	24.8*							
Cat 3 (case 2)	NM	IAV	21.2*	32.5	30.3	30.5	33.5	–	NA	NA	
		H5 subtype	21.7*	36.5	33.4	32.5	35.6				
		H5 2.3.4.4b	22.0*	–	33.2	32.8	–				
Cat 4 (case 2)	NM	IAV	25.1*	32.7	34.4	28.3	34.1	–	NA	NA	
		H5 subtype	25.7*	37.9	36.9	31.9	–				
		H5 2.3.4.4b	25.7*	36.3	37.1	31.6	–				
Cat 5 (case 3)	MN	IAV	NA	NA	NA	36.1*	NA	NA	36.6	–	
		H5 subtype							36.2		
		H5 2.3.4.4b							37.2		
Cat 6 (case 3)	MN	IAV	NA	NA	NA	34.1*	NA	NA	30.8	31.7	
		H5 subtype							32.0	33.7	
		H5 2.3.4.4b							33.2	34.8	

– = not detected; IAV = influenza A virus; NA = not available.

\* Results from the National Veterinary Services Laboratories (NVSL), Ames, IA, USA.

† Oropharyngeal swab collected in PBS.

NP antigens were detected by ELISA in cat 5 (S:N 0.501) and not in cat 6 (S:N 0.934).

## Discussion

The 4 cats that were autopsied had minimal or non-diagnostic gross lesions (notably mild subcutaneous and meningeal hemorrhages in cats 1 and 2). Yet, all 4 cats had histologic lesions that were striking in the brain and more subtle in the lung, which consisted of mononuclear and necrotizing encephalitis, interstitial pneumonia, and vasculitis in both organs, similar to those described in previous H5N1 infections in cats,<sup>13–15,23,25,29</sup> including the most recent clade 2.3.4.4b.<sup>24</sup> Similar to previous reports of clade 2.3.4.4b in cats,<sup>9,24</sup> brain was the most severely affected organ, and harbored a higher amount of IAV nucleic acid and NP antigen in all cats. Lung lesions appeared more acute in cats 1 and 2 and were mainly attributed to vascular damage with leakage of fibrin associated with the presence of IAV NP by IHC. Pulmonary changes appeared to be more chronic and subtle in cats 3 and 4 in which viral detection was confirmed by RT-rfPCR but not by IHC. Foci of necrosis and concurrent detection of IAV antigen have been reported in a variety of systemic organs in recent<sup>24</sup> and past<sup>14,23,25,29</sup> H5N1 infections in cats. In our cases, the 2 cats from Texas had multifocal myocardial necrosis associated with detection of IAV NP, similar to reports in several wild mammals naturally infected with H5N1 2.3.4.4b<sup>10</sup> and in cats experimentally infected with A/Vietnam/1194/2004(H5N1).<sup>23</sup> One cat from New Mexico also had a focus of myocarditis, but it was not associated with

detection of IAV NP by IHC. A few small foci of necrosis were also observed in the liver and adrenal gland of one cat. Unlike previous reports,<sup>14,23–25,29</sup> this lesion was not associated with immunoreactivity for IAV, and we did not identify necrosis or immunoreactivity in other organs, such as pancreas<sup>24</sup> or kidney.<sup>23–25</sup>

To our knowledge, IAV and associated lesions have not been reported in the salivary glands of cats, nor has a case series been reported with associated lesions in the eyes.<sup>4</sup> We retrieved no cases of feline sialadenitis or chorioretinitis due to IAV in a search of Google, PubMed, CAB Direct, Web of Science, and Scopus, using search terms “cat”, “feline”, “influenza”, “HPAI”, “H5N1”, “retinitis”, “chorioretinitis”, and “sialadenitis,” suggesting that these conditions have not been reported in cats. In addition to neurologic signs, blindness was reported in cats from the farms in Texas and New Mexico, and one cat from each farm had microscopic changes of segmental-to-disseminated chorioretinitis associated with intralésional IAV antigen, indicating the ability of this virus to infect all layers of the retina with subsequent clinical blindness. Interestingly, although conjunctivitis has been reported in people infected with H5N1 clade 2.3.4.4b,<sup>28</sup> conjunctivitis was not a feature in our feline cases. Cat 3 had multifocal necrosis in the submandibular salivary gland and the minor salivary glands of the tongue associated with immunodetection of IAV NP; cat 4 had mild perivascular lymphocytic sialadenitis with negative IAV immunodetection. The findings in cat 3 are particularly interesting because, along with the data in cattle,<sup>4,19</sup> they suggest a tropism of this virus strain for the glandular epithelium and



may contribute, at least in part, to the viral detection in the oropharyngeal swabs. Additional studies focusing on the viral tropism for the glandular epithelium of different species are therefore warranted. Infection of tonsils has been reported in experimental infections with H5N1 in cats<sup>23,29</sup>; cat 3 in our series had severe necrotizing tonsillitis, although we did not confirm IAV NP by IHC in this location.

To help guide sample selection and diagnosis in live, clinically ill cats, oropharyngeal swabs, nasal swabs, fecal swabs, and urine collected postmortem from cats 3 and 4, and oropharyngeal swabs, EDTA blood, and serum from live clinically ill cats 5 and 6 were analyzed by RT-rtPCR. In addition, seroconversion for the IAV NP was evaluated in the serum samples from the 2 living cats. All oropharyngeal swabs and urine samples were positive by RT-rtPCR; lower amounts of IAV nucleic acids were detected in the nasal swabs, impairing IAV subtyping. All fecal swabs were negative. Oropharyngeal swabs have been reported to be suitable for detecting both clinical and subclinical H5N1 infection in naturally infected cats<sup>9,14,18</sup> and bobcats,<sup>10</sup> including the clade 2.3.4.4b virus,<sup>9,10</sup> as well as in experimentally infected cats.<sup>23,29</sup> Authors of one study investigated and confirmed H5N1 in cat urine by viral isolation<sup>25</sup>; others detected the virus in the kidney by viral isolation, IHC, or PCR, but did not evaluate urine samples.<sup>13,23,24,29</sup> Although viral detection and isolation from nasal swabs and fecal or intestinal samples has been variably demonstrated in natural<sup>25,31</sup> and experimental<sup>13,23,29</sup> infections with H5N1 viruses in cats, including the outbreak in Poland,<sup>9</sup> the high Ct values in the nasal swabs and negative results in fecal samples in our study corroborate the reports of H5N1 2.3.4.4b infection in domestic cats in the United States<sup>24</sup> and France.<sup>3</sup> In both cases,<sup>3,24</sup> the virus was detected in 2 of 3 nasal swabs with Ct values >33.0, and was not detected in the 2 fecal samples collected.

In the experimental studies that detected H5N1 virus in rectal swabs and intestine by viral isolation or PCR procedures,<sup>13,23,29</sup> IHC detection was not observed or reported in any segment of the gastrointestinal tract, and viral titers in the rectal swabs varied widely compared to more consistent titers in the pharyngeal and nasal swabs in one study.<sup>23</sup> In cat 3, detection of IAV NP was suspected in small clusters of cellular debris lining the mucosal epithelium of the large intestine; however, no significant lesions were observed in the intestinal mucosa and lamina propria and viral nucleic acids were not detected in the corresponding fecal sample, suggesting a nonspecific reaction. All other gastrointestinal tissue sections examined had no immunoreactivity.

Our results, coupled with other reports, suggest that oropharyngeal swabs and urine are more reliable samples for RT-rtPCR detection of H5N1 2.3.4.4b, compared to nasal swabs and fecal swabs. However, the stage of clinical infection, potentially influencing the presence and amounts of virus in these samples, should be considered. Additional studies are needed to elucidate the routes and duration of viral shedding in cats and other animals infected with H5N1 clade 2.3.4.4b. In experimental studies with other H5N1

virus strains,<sup>13,23,29</sup> the virus was detected in pharyngeal, nasal, and rectal swabs of cats as early as 1 dpi and up to the end of the experiment at 7 dpi.

Cat 5 was the only cat evaluated serologically that was found to have antibodies to IAV NP by ELISA. Cat 6 had no seroconversion and lower Ct values in the oropharyngeal swab, EDTA whole blood, and serum sample, compared to cat 5. Cat 5 developed clinical signs first, followed by cat 6 on the next day, and all samples were collected on the day of onset of clinical signs in cat 6. To our knowledge, cat 5 (5-y-old) recovered and was still alive at the time of manuscript submission. Cat 6 (13-y-old) died 5 d after the onset of clinical disease and sample collection. Cat 5 may have been infected earlier than cat 6, and was thus further along in the disease process, and would have lower amounts of nucleic acids in these samples coupled with the presence of circulating antibodies. In cats experimentally infected with H5N1 and that displayed clinical signs starting at 2–4 dpi, antibodies against IAV NP were detected by ELISA as early as 14 dpi, but no serologic data between 0 and 14 dpi were available.<sup>29</sup> Seroconversion in subclinical cats was also demonstrated in the same study in cats infected with a lower viral dose ( $10^4$  EID) at 14 and 21 dpi, but not in cats inoculated with  $10^2$  and 1 EID.<sup>29</sup> In addition, seroconversion in subclinical cats was detected by a hemagglutination inhibition test in 2 of 40 cats from a natural outbreak in which cats were in contact with H5N1-infected birds, at 22 d after the death of the first positive bird.<sup>18</sup> Additional work is needed to further understand the timeframe between initial infection to seroconversion in cats that survive peracute disease. Additionally, development of an IAV ELISA specific to H5 may help reduce potential false-positive results arising from infection with other IAV subtypes.

Although cats 1–4 from Texas and New Mexico reportedly foraged on mice, rats, and birds, and were offered milk and colostrum from infected dairy cows, cats 5 and 6 from Minnesota were reportedly kept indoors and only had contact with people working at the affected dairy farm. Historically, infection with H5N1 in cats and other felids was mainly attributed to ingestion or direct and indirect contact with infected birds.<sup>12,14,18,27,31</sup> However, cat-to-cat transmission was also demonstrated to occur in experimentally infected cats<sup>15,23</sup> and postulated in naturally infected tigers kept in a tiger zoo.<sup>26</sup> Our findings raise the concern for transmission of H5N1 virus to cats, not only by ingestion of infected material, such as milk or dead birds, but also by contact with fomites or infected material transmitted via the cats' human handlers, such as owners, keepers, or caregivers. The infection status of the cats' owners in case 3 is unknown. Overall, a deeper understanding of viral transmission among a higher number of animals and a variety of hosts, from an epidemiologic point of view, is needed. Additional studies investigating the occurrence of horizontal transmission, including contact with body secretions (e.g., saliva, urine), are also warranted. Although a few HPAI H5N1 infections in humans have been reported since 2022,<sup>6,8,21,28</sup> HPAI is a zoonotic disease and close or prolonged, unprotected contact with



infected animals, contaminated environments (e.g., litter), or clinical samples can pose a risk of infection for people.<sup>8</sup>

### Acknowledgments

We thank the faculty and staff at the ISU-VDL who contributed to the processing and analysis of clinical samples in our investigation.

### Declaration of conflicting interests


The authors declared no potential conflicts of interest with respect to the research, authorship, and/or publication of this article.

### Funding


The authors received no financial support for the research, authorship, and/or publication of this article.

### ORCID iDs

Marta Mainenti  <https://orcid.org/0000-0001-8967-0016>

Christopher Siepker  <https://orcid.org/0000-0001-8590-046X>

Phillip Gauger  <https://orcid.org/0000-0003-2540-8769>

David Baum  <https://orcid.org/0000-0002-7094-8046>

Eric R. Burrough  <https://orcid.org/0000-0003-4747-9189>

### References

- Agüero M, et al. Highly pathogenic avian influenza A(H5N1) virus infection in farmed minks, Spain, October 2022. *Euro Surveill* 2023;28:2300001.
- Bevins SN, et al. Intercontinental movement of highly pathogenic avian influenza A(H5N1) clade 2.3.4.4 virus to the United States, 2021. *Emerg Infect Dis* 2022;28:1006–1011.
- Briand F-X, et al. Highly pathogenic avian influenza A(H5N1) clade 2.3.4.4b virus in domestic cat, France, 2022. *Emerg Infect Dis* 2023;29:1696–1698.
- Burrough ER, et al. Highly pathogenic avian influenza A(H5N1) clade 2.3.4.4b virus infection in domestic dairy cattle and cats, United States, 2024. *Emerg Infect Dis* 2024;30:1335–1343.
- Caliendo V, et al. Transatlantic spread of highly pathogenic avian influenza H5N1 by wild birds from Europe to North America in 2021. *Sci Rep* 2022;12:11729.
- Centers for Disease Control and Prevention (CDC), U.S. CDC technical report: highly pathogenic avian influenza A(H5N1) viruses. 2024. [cited 2024 Jul 11]. <https://www.cdc.gov/bird-flu/php/technical-report/h5n1-06052024.html>
- Centers for Disease Control and Prevention (CDC), U.S. H5N1 bird flu detections across the United States in backyard and commercial poultry. 2024. [cited 2024 Jul 26]. <https://stacks.cdc.gov/view/cdc/159002>
- Centers for Disease Control and Prevention (CDC), U.S. Highly pathogenic avian influenza A(H5N1) virus in animals: interim recommendations for prevention, monitoring, and public health investigations, 2024. [cited 2024 Aug 26]. <https://www.cdc.gov/bird-flu/prevention/hpai-interim-recommendations.html>
- Domańska-Blicharz K, et al. Outbreak of highly pathogenic avian influenza A(H5N1) clade 2.3.4.4b virus in cats, Poland, June to July 2023. *Euro Surveill* 2023;28:2300366.
- Elsmo EJ, et al. Highly pathogenic avian influenza A(H5N1) virus clade 2.3.4.4b infections in wild terrestrial mammals, United States, 2022. *Emerg Infect Dis* 2023;29:2451–2460.
- Frymus T, et al. Influenza virus infections in cats. *Viruses* 2021;13:1435.
- Keawcharoen J, et al. Avian influenza H5N1 in tigers and leopards. *Emerg Infect Dis* 2004;10:2189–2191.
- Kim HM, et al. Greater virulence of highly pathogenic H5N1 influenza virus in cats than in dogs. *Arch Virol* 2015;160:305–313.
- Klopfleisch R, et al. Distribution of lesions and antigen of highly pathogenic avian influenza virus A/Swan/Germany/R65/06 (H5N1) in domestic cats after presumptive infection by wild birds. *Vet Pathol* 2007;44:261–268.
- Kuiken T, et al. Avian H5N1 influenza in cats. *Science* 2004;306:241.
- Lee K, et al. Highly pathogenic avian influenza A(H5N6) in domestic cats, South Korea. *Emerg Infect Dis* 2018;24:2343–2347.
- Leguia M, et al. Highly pathogenic avian influenza A (H5N1) in marine mammals and seabirds in Peru. *Nat Commun* 2023;14:5489.
- Leschnik M, et al. Subclinical infection with avian influenza A (H5N1) virus in cats. *Emerg Infect Dis* 2007;13:243–247.
- Nelli RK, et al. Sialic acid receptor specificity in mammary gland of dairy cattle infected with highly pathogenic avian influenza A(H5N1) virus. *Emerg Infect Dis* 2024;30:1361–1373.
- Pohlmann A, et al. Has epizootic become enzootic? Evidence for a fundamental change in the infection dynamics of highly pathogenic avian influenza in Europe, 2021. *mBio* 2022;13:e0060922.
- Pulit-Penalzo JA, et al. Highly pathogenic avian influenza A(H5N1) virus of clade 2.3.4.4b isolated from a human case in Chile causes fatal disease and transmits between co-housed ferrets. *Emerg Microbes Infect* 2024;13:2332667.
- Puryear W, et al. Highly pathogenic avian influenza A(H5N1) virus outbreak in New England seals, United States. *Emerg Infect Dis* 2023;29:786–791.
- Rimmelzwaan GF, et al. Influenza A virus (H5N1) infection in cats causes systemic disease with potential novel routes of virus spread within and between hosts. *Am J Pathol* 2006;168:176–183.
- Sillman SJ, et al. Naturally occurring highly pathogenic avian influenza virus H5N1 clade 2.3.4.4b infection in three domestic cats in North America during 2023. *J Comp Pathol* 2023;205:17–23.
- Songserm T, et al. Avian influenza H5N1 in naturally infected domestic cat. *Emerg Infect Dis* 2006;12:681–683.
- Thanawongnuwech R, et al. Probable tiger-to-tiger transmission of avian influenza H5N1. *Emerg Infect Dis* 2005;11:699–701.
- Thiry E, et al. Highly pathogenic avian influenza H5N1 virus in cats and other carnivores. *Vet Microbiol* 2007;122:25–31.
- Uyeki TM, et al. Highly pathogenic avian influenza A(H5N1) virus infection in a dairy farm worker. *N Engl J Med* 2024;390:2028–2029.
- Vahlenkamp TW, et al. Protection of cats against lethal influenza H5N1 challenge infection. *J Gen Virol* 2008;89:968–974.
- Vreman S, et al. Zoonotic mutation of highly pathogenic avian influenza H5N1 virus identified in the brain of multiple wild carnivore species. *Pathogens* 2023;12:168.
- Yingst SL, et al. Qinghai-like H5N1 from domestic cats, northern Iraq. *Emerg Infect Dis* 2006;12:1295–1297.